

Electrocatalytic activity of the bimetallic Pt-Ru catalysts doped TiO₂-hollow sphere nanocomposites

In-Ho Lee, Hai-Doo Kwen and Seong-Ho Choi*

Department of Chemistry, Hannam University, Daejeon 305-811, Korea

(Received December 13, 2012; Revised January 16, 2013; Accepted January 16, 2013)

Pt-Ru@TiO₂-H 나노구조체촉매의 합성 및 전기화학적 특성평가

이인호 · 권해두 · 최성호*

한남대학교 화학과

(2012. 12. 13. 접수, 2013. 1. 16. 수정, 2013. 1. 16. 승인)

Abstract: This paper describes the electrocatalytic activity for the oxidation of small biomolecules on the surface of Pt-Ru nanoparticles supported by TiO₂-hollow sphere prepared for use in sensor applications or fuel cells. The TiO₂-hollow sphere supports were first prepared by sol-gel reaction of titanium tetraisopropoxide with poly(styrene-*co*-vinylphenylboronic acid), PSB used as a template. Pt-Ru nanoparticles were then deposited by chemical reduction of the Pt⁴⁺ and Ru³⁺ ions onto TiO₂-hollow sphere (Pt-Ru@TiO₂-H). The prepared Pt-Ru@TiO₂-H nanocomposites were characterized by transmission electron microscopy (TEM), X-ray diffraction (XRD), and elemental analysis. The electrocatalytic efficiency of Pt-Ru nanoparticles was evaluated via ethanol, methanol, dopamine, ascorbic acid, formalin, and glucose oxidation. The cyclic voltammograms (CV) obtained during the oxidation studies revealed that the Pt-Ru@TiO₂-H nanocomposites showed high electrocatalytic activity for the oxidation of biomolecules. As a result, the prepared Pt-Ru catalysts doped onto TiO₂-H sphere nanocomposites supports can be used for non-enzymatic biosensor or fuel cell anode electrode.

요약: 이 논문은 센서 및 연료전지에 사용할 수 있는 Pt-Ru@TiO₂-H 나노구조체촉매의 제조 및 전기화학적 촉매의 특성에 대한 것이다. 이 Pt-Ru@TiO₂-H 나노구조체촉매는 주형제인 폴리스티렌렌볼(PSB)을 제조하고, 이 주형제의 표면에 졸-겔 반응을 통해 TiO₂를 코팅한 후, Pt⁴⁺와 Ru³⁺의 환원에 의해 제조하였다. 제조된, Pt-Ru@TiO₂-H 나노구조체촉매는 전자투과현미경(TEM), X-선 회절(XRD)와 원소분석에 의해 특성평가하였고, Pt-Ru@TiO₂-H의 전기화학적 촉매특성은 에탄올, 메탄올, 도파민, 아스코르브 산, 프로말린과 글루코오스의 산화-환원 능력에 의해 평가 하였다. 이 Pt-Ru@TiO₂-H 나노구조체촉매는 바이오분자에 대해 전기화학적촉매 특성을 나타내어, 연료전지 전극 또는 비효소바이오센서에 사용 될 것으로 기대된다.

Key words: Electrocatalytic oxidation, Pt-Ru nanocomposites, TiO₂-Hollow nanocomposites, Poly(styrene-*co*-vinylphenylboronic acid)

★ Corresponding author

Phone : +82-(0)42-629-8824 Fax : +82-(0)42-629-8811

E-mail : shchoi@hnu.kr

1. Introduction

The electrocatalytic oxidation of organic compounds at noble metal electrodes using metal catalysts has been studied extensively for their applications in catalysis, fuel cells and sensors.¹⁻³ Pt and Pt-based alloy catalysts have been widely used for those catalysts.^{4,5} For example, initial research developing non-enzymatic sensors focused on the use of nanocrystalline metals, such as Pt or Au, especially Pt-based amperometric electrodes.^{6,7} The desire for better and cheaper electrocatalysts has resulted in bimetallic systems being developed. Pt-Au,⁸ Pt-Pb,⁹⁻¹² and Pt-Ru¹³ are widely used for applications because they often exhibit better catalytic properties than their monometallic counterparts.^{14,15} For instant, bimetallic catalysts such as Pt-Ru are considered the most effective catalysts for the methanol oxidation reaction¹⁶⁻¹⁸ due to their formation of two kinds of site on the catalyst surface: Pt site with high activity toward the dehydrogenation process and Ru site providing the necessary oxygen species, e.g., weakly bound OH groups or adsorbed water molecules.

In fact, a suitable supporting material is important to affect the performance of supported electrocatalysts owing to interactions and surface reactivity.^{19,20} Many research efforts have been devoted to improving the catalytic performance of carbon supported Pt-Ru catalysts.²¹⁻²³ In a colloidal method, dispersion and adsorption of catalytic nanoparticles on the surface of carbon-supports is done in the presence of protecting agents to avoid aggregation of particles. It should be noted that the protecting agent is likely to reduce the catalytic activities of catalyst particles. In another method known as the impregnation method, a metal precursor is reduced by the carbon supports dispersed in a solution.²⁴⁻²⁶ In previous papers,^{27,28} the Pt-Ru nanoparticles were deposited on various carbon-supports using γ -irradiation to use as anode catalysts in a direct methanol fuel cell (DMFC). However, the life time of the electrode was reduced since the carbon supports were slowly oxidized in the fuel cell.

On the other hand, oxide materials are widely used

as a support in heterogeneous catalyst since they have high surface area, uniform porous structure, low electrical resistance, effective interactions between catalysts and supports, and inherently higher stability compared to carbon in oxidizing environments.^{29,30} The use of titanium dioxide support in a fuel cell operation has been of great interest due to its stability, low cost, commercial availability in water, and ease to control size and structure.^{31,32} The potential applications of hollow nanomaterials, especially TiO₂ hollow (TiO₂-H) spheres, have been explored in various areas, such as light-trapping, chemical separation, photocatalysts, bio-medicine, and optical devices.^{33,34} Compared to general core-shell nanostructures, TiO₂-H spheres are exceptional for their special internal cavity, high specific surface area, high mobility, and low density.³⁵⁻³⁷

TiO₂-H sphere was successfully prepared using poly(styrene-*co*-vinylphenylboronic acid), PSB, as a template by using a sol-gel method. Previous studies^{38,39} reported the preparation of core-shell conductive balls with polystyrene (PS) as a core and polypyrrole (PPy) as a shell by *in situ* polymerization of pyrrole. Surfactants including sodium dodecyl sulfite and PVP were needed to modify the hydrophobic surface of PS and help in the formation of a shell layer of PPy over the surface of the PS particles. On the other hand, to avoid using surfactants, a PS core was copolymerized with a hydrophilic group like anhydride, boronic acid, carboxylic acid, or sulfonate groups prior to the core-shell reaction.

In this study, we focused on the application of Pt-Ru@TiO₂-H sphere nanocomposites for the detection of multiple biomolecules. The monitoring of several (bio) chemical parameters is specially interesting in food analysis in which the samples contain a complex mixture of analytes of interest. For example, glucose, lactic acid, ethanol, etc. are produced in fermentation processes. Firstly, we synthesized a Pt-Ru@TiO₂-H sphere nanocomposites using PSB as a template (~320 nm) by chemical reduction. Subsequently, PSB/TiO₂ core-shell (TiO₂-CS) spheres were prepared by sol-gel reaction. Then the prepared TiO₂-H hollow spheres were annealed to remove the PSB template

at 450 °C under air atmosphere. In order to prepare the electrocatalysts, we deposited Pt-Ru nanoparticles on the surface of TiO₂-H by chemical reduction. Finally, the non-enzymatic sensor was fabricated by depositing the as-prepared Pt-Ru@TiO₂-H nanocomposites on the surface of a glassy carbon electrode (GCE), which was prepared by a hand casting method with Nafion solution as a binder. The electrocatalytic activity of Pt-Ru nanoparticles (NPs) on metal oxide supports was evaluated via small bio molecules, such as ethanol, methanol, dopamine, ascorbic acid, formalin, and glucose in 0.5 M H₂SO₄ electrolyte in order to use for a non-enzymatic biosensor or fuel cell anode electrode.

2. Experiment

2.1. Reagents

Styrene, polyvinylpyrrolidone (PVP), 4-vinylphenylboronic acid (VPBAC), titanium (IV) butoxide (TBT), potassium persulfate (K₂S₂O₈, KPS), H₂PtCl₆ × H₂O (37.5% Pt), RuCl₃ × H₂O (41.0% Ru), and Nafion (perfluorinated ion-exchange resin, 5% (w/v) in 90% aliphatic alcohol/10% water solution) were purchased from Sigma-Aldrich Co. (Korea) and used without further purification. Solutions for the experiments were prepared with water purified in a Milli-Q plus water purification system (Millipore Co. Ltd.; the final resistance of water was 18.2 MΩcm⁻¹) and

degassed prior to each measurement. All other chemicals were of reagent grade, and were used without further purification.

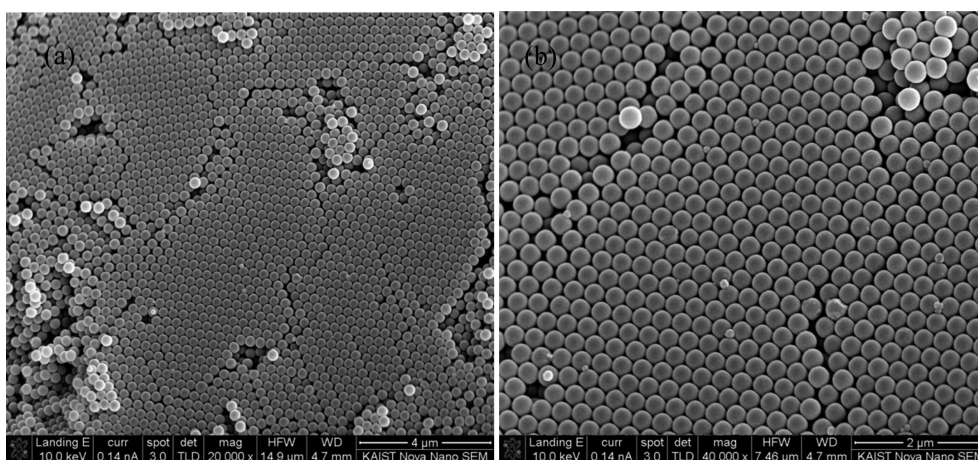
2.2. Synthesis of PSB as core-ball via surfactant-free emulsion polymerization

PSB spheres as core-ball were prepared as follows: The reaction mixture of styrene and VPBAC was prepared in deionized (D.I.) water prior to the polymerization performed using KPS as an initiator at 75 for 24 hfh by stirring at 350 rpm under a nitrogen atmosphere.

2.3. Preparation and characterization of the Pt-Ru@TiO₂-H catalysts

Fig. 1 shows a schematic of the preparation of the Pt-Ru@TiO₂-H nanocomposite for use as a biosensor. To prepare the TiO₂-H spheres, the PSB was coated with TiO₂ NPs by sol-gel method. The prepared PSB (0.5 g) and PVP (0.75 g) were dissolved in 120 mL of ethanol. The dispersed solution of TBT/EtOH (10 vol%,) was then added to the PVP-coated PSB solution. Finally, 5.0 mL of D.I. water was added to the reaction solution to induce surface dehydrogenation of the TiO₂ NPs. The TiO₂-H spheres were obtained by calcination at 450 °C for 4 hfh in air.

To prepare the electrocatalyst, bimetallic Pt-Ru NPs were deposited onto the surface of TiO₂-H spheres by chemical reduction. The TiO₂-H spheres



Scheme 1. Preparation process of Pt-Ru catalysts based on the hollow TiO₂ supports.

were dispersed in 120 mL of aqueous ethylene glycol (3:1 volume ratio of ethylene glycol and H₂O). Subsequently, H₂PtCl₆ (0.293 g) and RuCl₃ (0.197 g) were added to the reaction solution, and the metallic ions reduced at 130 for 12 hfh to obtain the Pt-Ru@TiO₂-H nanocomposites.

The particle size and morphology of the PSB, TiO₂-CS, TiO₂-H and Pt-Ru@TiO₂-H catalysts were analyzed by field-emission scanning electron microscopy (FE-SEM, Hitachi, S-4700, Japan), and high-resolution transmission electron microscopy (HR-TEM, JEOL, JEM-2010, USA). Mean diameters and size distributions were further determined by elastic light scattering (ELS, ELS-8000, Otsuka Co., Japan). The content of Pt and Ru in samples was measured by the energy dispersive X-ray (EDX) analyzer combined with HR-TEM. X-ray diffraction (XRD) patterns were obtained using a Japanese Rigaku D/max γ A X-ray diffractometer equipped with graphite mono-chromatized Cu K α radiation ($\lambda=0.15414$ nm). The scanning range was 5-80° with a scanning rate of 5°/min.

2.4. Fabrication of non-enzymatic biosensors based on Pt-Ru@TiO₂-H sphere catalysts

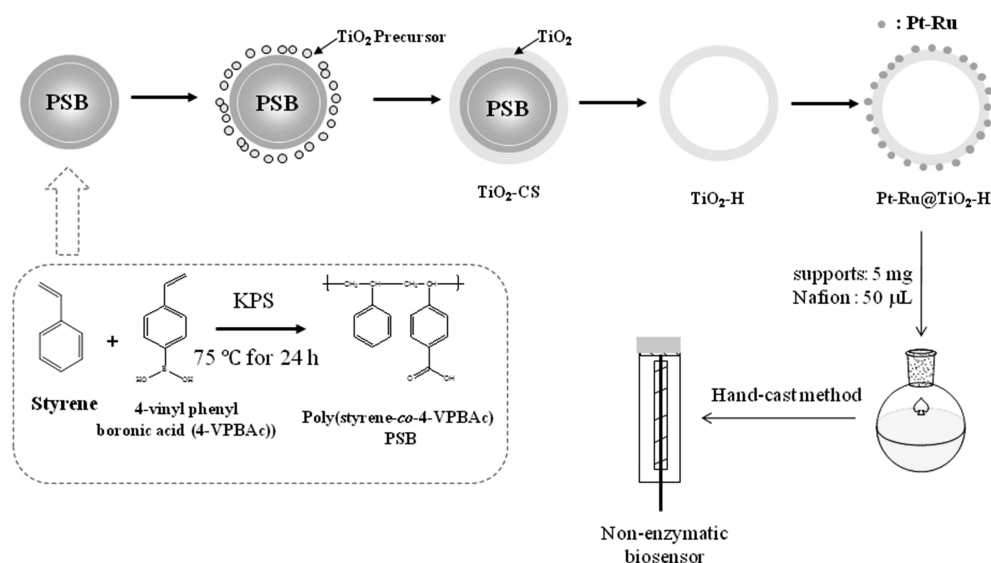
To evaluate the catalytic efficiency of Pt-Ru@TiO₂-

H sphere catalysts for the electro-oxidation of ethanol, methanol, dopamine, ascorbic acid, formalin, and glucose, the catalyst electrode was prepared as follows: Firstly, the catalytic inks were prepared by mixing of catalysts (5.0 mg) and 5% Nafion solution (0.05 mL) and stirred for 24 hfh. Secondly, the catalytic inks were applied on a glass carbon (GC) (0.02 cm²) by wet coating, and dried in a vacuum oven at 50 °C under nitrogen gas. The electro-oxidation of each target molecule was examined using the Pt-Ru@TiO₂-H catalyst electrode, submerged in 0.5M H₂SO₄ electrolyte by cyclic voltammetry (EG&G INSTRUMENTS, Potentiostat/Galvanostat model 283, USA).

3. Results and discussion

3.1. Characterization of Pt-Ru @TiO₂-H catalysts

PSB was prepared by emulsion-free copolymerization of styrene and VPBAc and used as a template for preparing nanostructure supports, as shown in *Scheme 1*. To avoid using surfactant for core-shell preparation, a PS core was copolymerized with a hydrophilic group which was boronic acid prior to the core-shell reaction. The boronic acid group that



Scheme 1. Preparation process of Pt-Ru catalysts based on the hollow TiO₂ supports.

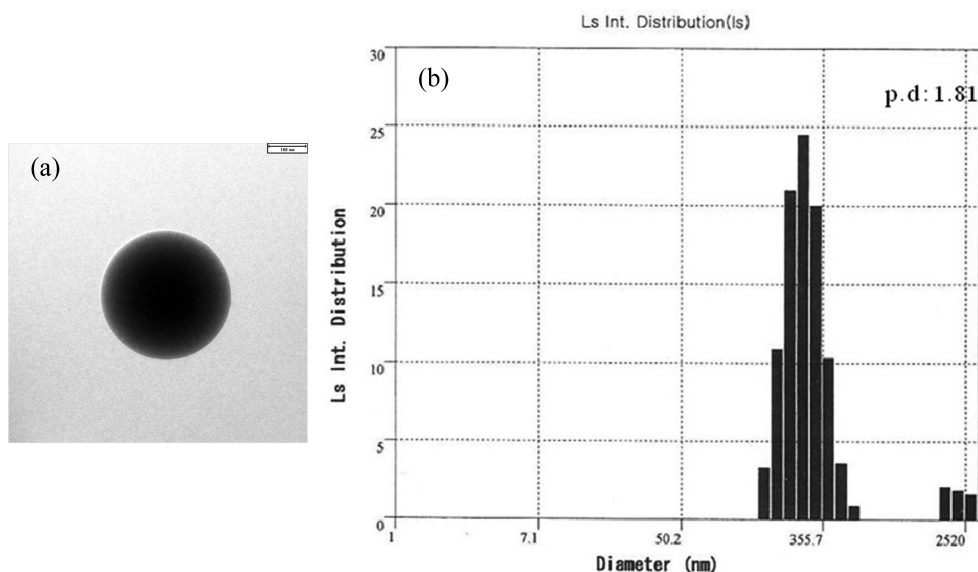


Fig. 2. TEM image (a) and ELS data (b) of PSB spheres prepared by emulsion-free polymerization.

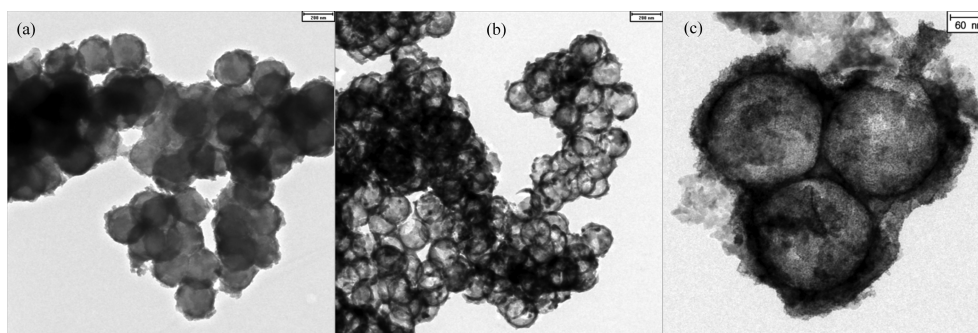


Fig. 3. TEM images of the TiO_2 -CS before calcinations (a), TiO_2 -H after calcinations at $550\text{ }^\circ\text{C}$ (b), and Pt-Ru@ TiO_2 -H (c).

was present on the PSB surface was expected to have stronger interactions with titanium alkoxide. The SEM images in Fig. 1 show PSB templates that are spherical with a uniform size of approximately 300 nm in average diameter. Size distribution of PSB determined by ELS shows similar to the particle size measured by TEM, as shown in Fig. 2.

Fig. 3 shows the TEM images for TiO_2 /PSB-CS (a), TiO_2 -H (b), and Pt-Ru@ TiO_2 -H (c) nanocomposites. The average external diameter of the hollow microspheres was $\sim 325\text{ nm}$ (Fig. 3(a)), and the average shell thickness of the hollow microspheres was about 37 nm. After being calcined at $550\text{ }^\circ\text{C}$, the morphology and mean external diameter of the

hollow microspheres remained almost same (Fig. 3 (b)), which demonstrated their thermal stability. Pt-Ru@ TiO_2 -H showed a very similar morphology and size (Fig. 3(c)). Although Pt-Ru NPs did not completely appear in the TEM image, the presence of Pt-Ru NPs on TiO_2 -H was confirmed by EDX (Fig. 4). The sample exhibited a Pt:Ru atomic ratio of approximately 68:32 (14.6:6.9 wt.%), which differed from the nominal Pt:Ru atomic ratio of 1:1 used in the preparation. This is because some Ru^{3+} ions failed to be simultaneously reduced with Pt^{4+} ions within the reaction time since the redox potential of Ru^{3+}/Ru ($E_0 \sim 0.84\text{ V}$) is of much lower than that of Pt^{4+}/Pt ion ($E_0 \sim 1.41\text{ V}$).⁴⁰

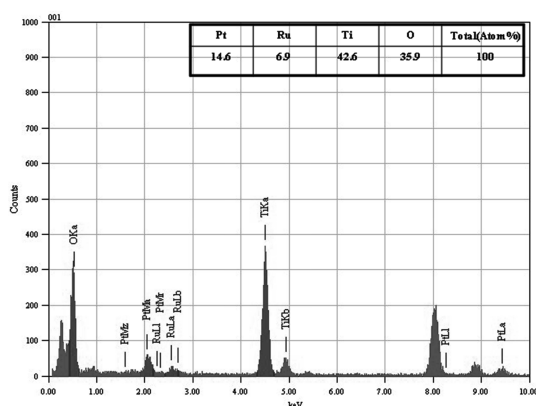


Fig. 4. EDX data of Pt-Ru@TiO₂-H spheres.

Fig. 5 presents XRD patterns of the TiO₂-H and Pt-Ru@TiO₂-H catalysts. The synthesized TiO₂-H microsphere after calcination is shown in Fig. 5(a). After calcination at 550 for 2 hfh, the strong and sharp diffraction peaks indicated that the product was highly crystalline and was indexed perfectly to the anatase phase of TiO₂ (JCPDS 21-1272). The TiO₂-H was further modified with Pt and Ru doping. As shown in Fig. 5(b), the XRD pattern of TiO₂-H after Pt-Ru doping displays a set of widened peaks at 39.9°, 46.2°, and 67.4°, in addition to those of anatase TiO₂. They can be assigned as the Pt (111), (200), and (220) planes, respectively, of the face centered cubic structure of Pt and Pt alloy particles. XRD peaks corresponding to metallic Ru or to any other Ru-rich materials do not appear in this sample. However, some oxide form of Ru may present in the amorphous state.^{41,42} Those results confirmed the successful preparation of the Pt-Ru@TiO₂-H nanocomposites by chemical reduction method.

3.2. Electrocatalytic efficiency of catalysts toward the oxidation of small molecules

The catalytic performance of TiO₂-H sphere supported Pt-Ru catalysts toward the electrochemical oxidation of small biomolecules was tested. Fig. 6 shows the cyclic voltammograms (CVs) of ethanol (a), methanol (b), dopamine (c), ascorbic acid (d), formalin (e), and glucose (f) oxidations with various

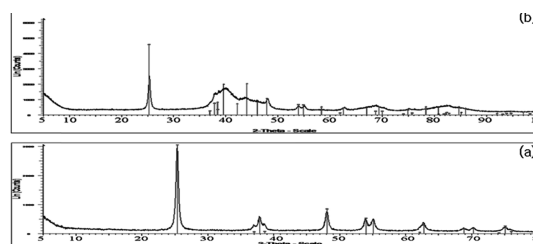


Fig. 5. XRD patterns of TiO₂-H spheres calcined at 550 °C (a) and Pt-Ru/TiO₂-H (b).

concentrations in 0.5 M H₂SO₄ electrolyte at a scan rate 50 mV/s. The concentration of ethanol is varied from 0.05 to 2 M and the peak current appears at 0.8 V (vs Ag/AgCl) corresponding to the oxidation of ethanol (Fig. 6(a)). The maximum catalytic efficiency is appeared in 0.5 M ethanol concentration. Fig. 6(b) presents the CVs for electro-oxidation of methanol in a concentration range from 0.05 to 2 M. The peak current appears at 0.7 V (vs Ag/AgCl) corresponding to the oxidation of 0.5 M methanol. The redox of dopamine involves two-proton and two-electron transferring processes.⁴³ Fig. 6(c) displays the CVs for different concentrations (5.0×10⁻⁴-0.10 M) of dopamine. The electrode exhibits a reversible electron process according to the dopamine concentration. The dopamine oxidation currents gradually increase with increasing concentration. The maximum current measured at 0.68 V (vs. Ag/AgCl) for the electro-oxidation of 0.05 M dopamine forming o-quinone in acidic media.⁴³ The electrooxidation of ascorbic acid (AA) on modified GCs with the catalysts was evaluated in various concentration of AA, as shown in Fig. 6(d). The anodic currents start to increase at around 0.3 V and continue to increase up to 1.2 V in the presence of 1.0 M AA. The catalyst in the presence of 1.0 M AA remarkably increased the oxidation currents compared to lower concentrations of AA present. The current values at 0.6 V in the positive scans were used to evaluate the activities for AA oxidation. Fig. 6(e) presents the CVs for electro-oxidation of formalin in a concentration range from 0.05 to 2 M. The formalin oxidation currents gradually increase with increasing concentration. The maximum current measured at 0.7 V (vs. Ag/AgCl) for the

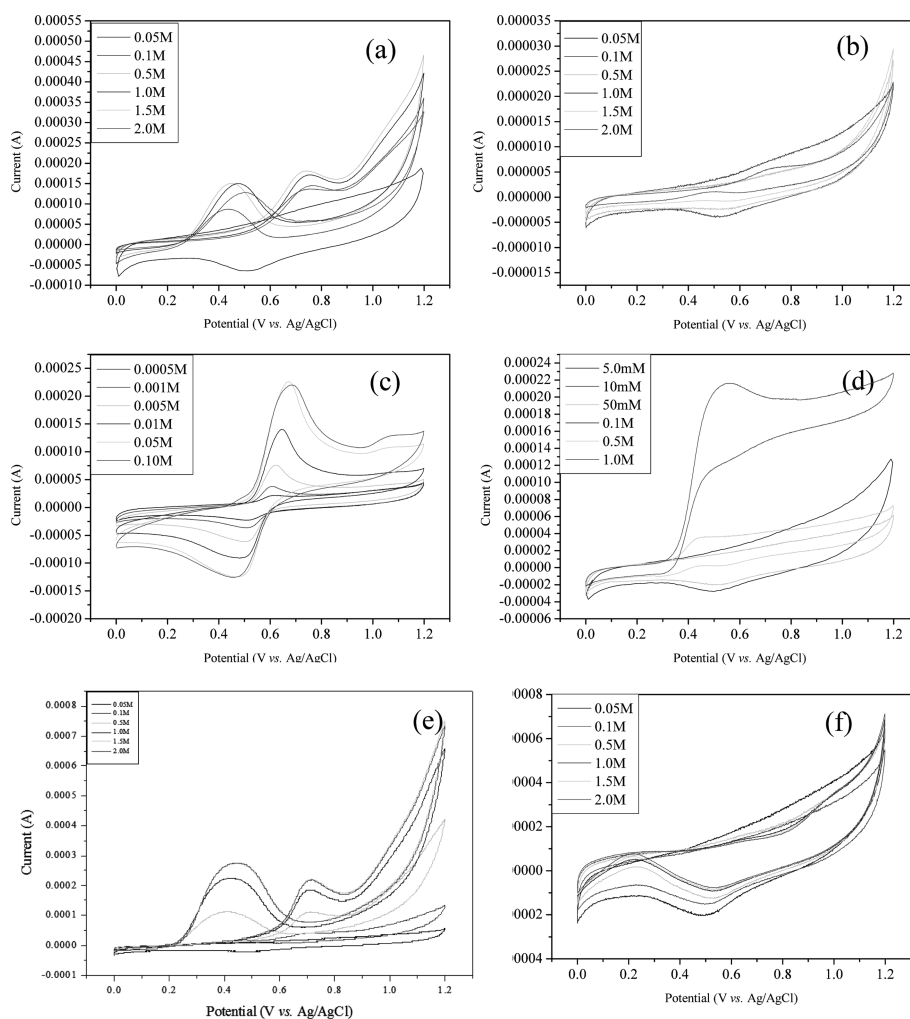


Fig. 6. Cyclic voltammograms of ethanol (a), methanol (b), dopamine (c), ascorbic acid (d), formalin (e), and glucose (f) oxidation on Pt-Ru@TiO₂-H catalysts modified electrode in 0.5 M H₂SO₄ at a scan rate 50 mV/s.

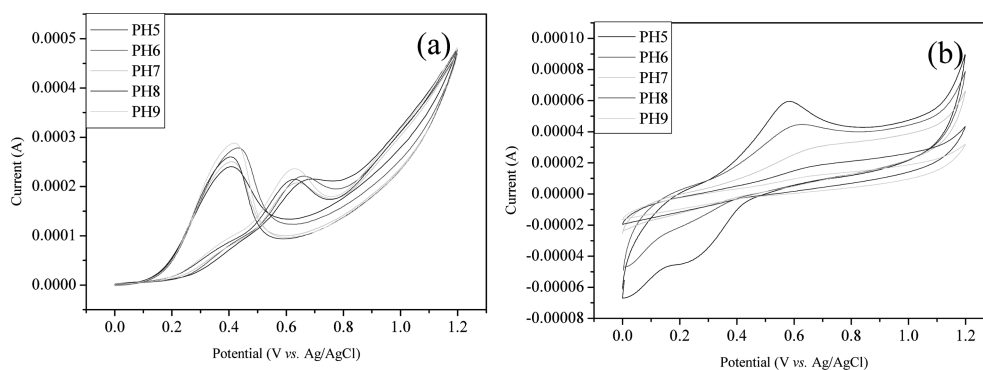


Fig. 7. Cyclic voltammograms (CV) of formalin oxidation (a) and dopamine oxidation (b) on Pt-Ru@TiO₂-H catalyst modified electrodes in pH (5-9) at a scan rate of 50 mV/s.

electro-oxidation of 2 M formalin. Fig. 6(f) shows the CVs of Pt-Ru@TiO₂-H sphere nanocomposites modified electrode in the presence of various concentrations of glucose. No redox peaks can be observed in the CV of the electrode suggesting that the catalysts cannot undergo the redox reaction in the potential range of interest.

Fig. 7(a) exhibits the CVs of the GCE modified by surface deposition of the Pt-Ru@TiO₂-H nanocomposites toward oxidation of 1.0 mM formalin (a) and 1.0 mM dopamine (b) as a function of pH. The sensing efficiency for formalin oxidation was not significantly affected by pH whereas for dopamine oxidation, the sensing efficiency increased as the pH decreased from 9.0 to 5.0. Consequently, pH 5.0 was chosen as the optimal pH.

The cyclic voltammograms (CV) obtained during the oxidation studies revealed that the Pt-Ru@TiO₂-H nanocomposites showed best catalytic function toward the oxidation of dopamine in acidic media. The Pt-Ru@TiO₂-H nanocomposite electrodes showed high electrocatalytic activity for the electro-oxidation of ethanol and formalin. However, the sensing efficiency of nanocomposites is needed to improve for the electro-oxidation of methanol, ascorbic acid and glucose.

4. Conclusion

In this paper, we have presented the preparation of bimetallic Pt-Ru catalysts doped TiO₂-H sphere nanocomposites and the results of electrocatalytic efficiency of the catalysts via ethanol, methanol, dopamine, ascorbic acid, formalin, and glucose oxidation. To prepare the electrocatalyst, bimetallic Pt-Ru nanoparticles were deposited onto the surface of TiO₂-H by chemical reduction. The sample exhibited that a Pt:Ru atomic ratio of approximately 68:32 (14.6:6.9 wt.%) was well deposited onto the anatase phase of TiO₂-H sphere nanocomposites. A non-enzymatic sensor was fabricated by depositing the as-prepared Pt-Ru@TiO₂-H nanocomposites on the surface of a GCE. The CVs obtained during the oxidation studies revealed the superior catalytic

function of the Pt-Ru@TiO₂-H nanocomposites toward the oxidation of dopamine. The Pt-Ru@TiO₂-H electrodes also showed the high electrocatalytic activity for electro-oxidation of ethanol and formalin. On the basis of the results, the prepared Pt-Ru catalysts doped onto TiO₂-H sphere nanocomposites supports can be used for non-enzymatic biosensor or fuel cell anode electrode.

Acknowledgement

This work was supported by the Hannam University Research Fund (2012).

References

1. G. S. Attard, P. N. Bartlett, N. R. B. Coleman, J. M. Elliott, J. R. Owen and J. H. Wang, *Sci.*, **278**, 838-840 (1997).
2. F. Leroux, B. E. Koene, L. F. Nazar, *J. Electrochem. Soc.*, **143**, L181-L183 (1996).
3. J. Wang and L. Agnes, *Anal. Chem.*, **64**, 456-459 (1992).
4. X. H. Xia, T. Iwasita, F. Ge and W. Vielstich, *Electrochim. Acta*, **41**, 711-718 (1996).
5. Z. Liu, X. Y. Ling, X. Su, J. Y. Lee and L. M. Gan, *J. Power Source*, **149**, 1-7 (2005).
6. S. J. Park, T. D. Chung and H. C. Kim, *Anal. Chem.*, **75**, 3046-3049 (2003).
7. Y. Y. Song, D. Zhang, W. Gao and X. H. Xia, *Chem. Eur. J.* **11**, 2177-2182 (2005).
8. A. Habrioux, E. Sibert, K. Servat, W. Vogel, K. B. Kokoh and N. Alonso-Vante, *J. Phys. Chem. B*, **111**, 10329-10333 (2007).
9. H. F. Cui, J. S. Ye, W. D. Zhang, C. M. Li, J. H. T. Luong and F. S. Sheu, *Anal. Chim. Acta*, **594**, 175-183 (2007).
10. Y. Bai, Y. Sun and C. Sun, *Biosens. Bioelectron.*, **24**, 579-585 (2008).
11. J. Wang and D. F. Thomas, *Chen. A. Anal. Chem.*, **80**, 997-1004 (2008).
12. Y. Sun, H. Buck and T. E. Mallouk, *Anal. Chem.*, **73**, 1599-1604 (2001).
13. F. Xiao, F. Zhao, Y. Zhang, G. Guo and B. Zeng, *J. Phys. Chem. C*, **113**, 846-849 (2009).

14. H. F. Cui, J. S. Ye, X. Liu, W. D. Zhang and F. S. Sheu, *Nanotechnology*, **17**, 2334-2339 (2006).
15. L. Qian and X. Yang, *J. Phys. Chem. B*, **110**, 16672-16678 (2006).
16. X. M. Ren, P. Zelenary, S. Thomas, J. Davey and S. Gottesfeld, *J. Power Sources*, **86**, 111-116 (2000).
17. Y. Y. Tong, H. S. Kim, P. K. Babu, P. Waszczuk, A. Wieckowski and E. Oldfield, *J. Am. Chem. Soc.*, **124**, 468-473 (2002).
18. C. Bock, C. Paquet, M. Couillard, G. A. Gotton and B. R. MacDougall, *J. Am. Chem. Soc.*, **126**, 8028-8037 (2004).
19. K. Park, Y. Sung, S. Han, Y. Yun and T. Hyeon, *J. Phys. Chem. B*, **108**, 939-944 (2004).
20. Z. Liu, J. Y. Lee, W. Chen, M. Han and L. M. Gan, *Langmuir*, **20**, 181-187 (2004).
21. Z. Liu, L. M. Gan, L. Hong, W. Chen and J. Y. Lee, *J. Power Source*, **139**, 73-78 (2005).
22. G. Chai, S. B. Yoon, S. Kang, J.-H. Choi, Y.-E. Sung, Y.-S. Ahn, H.-S. Kim and J.-S. Yu, *Electrochim. Acta*, **50**, 823-826 (2004).
23. D. F. Silva, A. O. Neto, E. S. Pino, M. Linardi and E. V. Spinace, *J. Power Source*, **170**, 303-307 (2007).
24. W. Chen, J. Y. Lee and Z. Liu, *Mater. Lett.*, **58**, 3166-3169 (2004).
25. Z. Liu, J. Y. Lee, W. Chen, M. Han and L. M. Gan, *Langmuir*, **20**, 181-187 (2004).
26. K.-D. Seo, S.-D. Oh, S.-H. Choi, S.-H. Kim, H. G. Park and Y. P. Zhang, *Colloids Surf. A*, **313**, 393-397 (2008).
27. H.-B. Bae, J.-H. Ryu, B.-S. Byun, S.-H. Choi, S.-H. Kim and C.-G. Hwang, *Adv. Mater. Res.*, **47-50**, 1478-1481 (2008).
28. H. Chhina, S. Campbell and O. Kesler, *J. Power Sources*, **161**, 893-900 (2006).
29. N. Zheng and G. D. Stuck, A general synthetic strategy for oxide-supported metal nanoparticle catalysts. *J. Am. Chem. Soc.*, **128**, 14278-12480 (2006).
30. H. Einaga and M. Harada, *Langmuir*, **21**, 2578-2584 (2005).
31. J. Tian, G. Sun, L. Jiang, S. Yan, Z. Mao and Q. Xin, *Electrochem. Commun.*, **8**, 1439-1444 (2006).
32. J. H. Pan, X. W. Zhang, A. J. Du, D. D. Sun and J. O. Leckie, *J. Am. Chem. Soc.*, **130**, 11256-11257 (2008).
33. H. J. Koo, Y. J. Kim, Y. H. Lee, W. I. Lee, K. Kim and N. G. Park, *Adv. Mater.*, **20**, 195-199 (2008).
34. S. S. K. Kamal, P. K. Sahoo, M. Premkumar, N. V. R. Rao, T. J. Kumar, B. Sreedhar, A. K. Singh, S. Ram and K. C. Sekhar, *Chem. J. Alloys Compd.*, **474**, 214-218 (2009).
35. J. G. Yu, W. Liu and H. G. Yu, *Cryst. Growth Des.*, **8**, 930-934 (2004).
36. Y. Wang, F. B. Su, J. Y. Lee and X. S. Zhao, *Chem. Mater.*, **18**, 1347-1353 (2009).
37. C. H. Chang, P. S. Son, J. A. Yoon and S. H. Choi, *J. Nanomater.*, **2010**, 1-13 (2010).
38. J. H. Chae, S. H. Jung and S. H. Choi, *Current Applied Physics*, **10**, S97-105 (2010).
39. F. A. Cotton; Wildinson, G. Advanced Inorganic Chemistry; John Wiley & Sons Inc.: New York, 1988.
40. B. Yang, Q. Lu, Y. Wang, L. Zhiang, J. Lu and P. Liu, *Chem. Mater.*, **15**, 3552-3579 (2003).
41. D. R. Rolison, P. L. Hagans, K. E. Swider and J. W. Long, *Langmuir*, **15**, 774-779 (1999).
42. S. Song, Q. Gao, K. Xia and L. Gao, *Electroanalysis*, **20**, 1159-1166 (2008).